

Some small weakly coordinating anions based on carboranes

Lauri Lipping^{*}, Ilmar A. Koppel, Ivar Koppel, and Ivo Leito

Department of Chemistry, University of Tartu, Jakobi 2, 51014 Tartu, Estonia

Received 11 May 2006

Abstract. The intrinsic gas-phase acidities of $\text{CB}_4\text{X}_n\text{H}_{5-n}\text{H}$ and $\text{CB}_5\text{X}_n\text{H}_{6-n}$ ($\text{X} \equiv \text{F}, \text{Cl}$ or CF_3) were calculated using the DFT B3LYP method at the 6-311+G** level. For comparison also the 6-31+G* basis set was used for fluorinated species. The results of the two calculation levels correlated satisfactorily. As the most favourable protonation site of these anions, the facet on the opposite side from the carbon-peaked polyhedron was found. When ordering the substituent groups in terms of increasing acidity of the carboranes, the order $\text{F} < \text{Cl} < \text{CF}_3$ was obtained.

Key words: carboranes, superacids, weakly coordinating anions.

INTRODUCTION

Weakly coordinating anions with very low nucleophilicity [1, 2] and extremely low proton affinity have been studied for some time because of the need for very stable counter-ions in a great variety of different chemical and electrochemical processes, which include efforts to create new catalysts, unstable cations, superstrong oxidants, acids, etc. Practical demands for the anions have already motivated the elaboration of systems like tetraphenylborate, perfluorotetraphenylborate, OTeF_5^- , and the derivatives of 1-carba-*closo*-dodecaborate ion [1].

At the moment the most promising class of weakly coordinating anions is the one that is based on the exceptionally stable cluster of boron atoms [3]. Usually these anions have a relatively regular spatial structure and the van der Waals radii beginning from around 0.3–0.5 nm. For describing the systems, analogy with benzene π -bonding and aromaticity has been used, which in the case of carboranes is expressed as σ -aromaticity [3]. The tangentially delocalized σ -bonds, which are the most stable bonds in chemistry, and a huge

^{*} Corresponding author, lauri.lipping@alecoq.ee

HOMO–LUMO gap turn the icosahedral cages into an extraordinarily stable system in the extreme conditions of electrophilic and oxidative reactivity [3].

For the first time $\text{CB}_{11}\text{H}_{12}^-$ was synthesized by Knoth in the 1960s [4]. Later, the method was improved and simplified [5, 6]. Although the chemistry of carboranes as anions has a relatively long (ca 40 years) history, the first actual carborane-based “weighable and measurable” superacids (i.e., conjugate acids of carborane anions) were synthesized and liberated by Reed and coworkers in 2000 [7–9]. Several attempts have been made to estimate either theoretically [2, 10, 11] or experimentally the intrinsic or solution-phase acidity of 1-carba-*closo*-dodecaborate carborane-based superacids [3, 9, 12].

Preliminary calculations [10, 11], made with the density functional theory (DFT) using the B3LYP exchange-correlation functional at the 3-21+G* and 6-31+G* levels and the PM3 semi-empirical method, showed that adding some electronegative substituents increases acidity, but also increases the tendency of the fragmentation of the boron cage.

In this communication we introduced into our agenda investigation of the basic features such as relative acidities and structures and stability of conjugate acids based on different carborane clusters smaller than 12-vertex $\text{CB}_{11}\text{H}_{12}^-$ with the standard basis set at the 6-311+G** level. The calculations of clusters reported in this study were performed using the Gaussian 03 system of programs.

THE APPROACH AND RESULTS

The DFT B3LYP/6-31+G* and 6-311+G** calculations were carried out on two different types of $\text{CB}_n\text{H}_{n+1}^-$ cages. Later these were used to model and calculate the corresponding fluorinated, chlorinated, and CF_3 -substituted anion derivatives and their conjugate acids.

Boron clusters were partitioned into belts of vertexes as 1:3:1 and 1:4:1. Replacement of hydrogens with substituents was done systematically beltwise, starting from the vertex antipodal to carbon.

For each cluster, depending on the size and extent of the substituents, 2–4 different protonation places were used to ascertain the most likely one. Gas-phase acidities (GA) of a neutral acid HA were calculated according to the thermodynamic heterolysis equilibrium:



where $\Delta G_{\text{acid}} \equiv \text{GA} \equiv \Delta G$. By definition, the gas-phase acidity of a neutral acid HA is equal to the gas-phase basicity toward the proton of its conjugate anion, A^- . These quantities provide valuable information about the intrinsic, solvent-independent properties of the acids.

Results are given in Tables 1 and 2 for the ΔG_{acid} values of intrinsic gas-phase acidities of the acid systems. More detailed information about the results of the DFT calculations is given in the Appendixes.

Table 1. ΔG_{acid} values (kcal/mol) of $\text{CB}_4\text{X}_5\text{H}$ and $\text{CB}_5\text{X}_6\text{H}$ based systems ($\text{X} \equiv \text{F}, \text{Cl}, \text{or } \text{CF}_3$) calculated at the DFT B3LYP/6-311+G** level (298 K)

1 : 3 : 1 acid	ΔG_{acid}	1 : 4 : 1 acid	ΔG_{acid}
$\text{CB}_4\text{H}_5\text{H}$	319.6	$\text{CB}_5\text{H}_6\text{H}$	305.1
$\text{CB}_4\text{F}_1\text{H}_4\text{H}$	314.9	$\text{CB}_5\text{F}_1\text{H}_5\text{H}$	301.9
$\text{CB}_4\text{F}_4\text{H}_1\text{H}$	307.1	$\text{CB}_5\text{F}_5\text{H}_1\text{H}$	285.1
$\text{CB}_4\text{F}_5\text{H}$	301.5	$\text{CB}_5\text{F}_6\text{H}$	278.6
$\text{CB}_4\text{Cl}_1\text{H}_4\text{H}$	308.9	$\text{CB}_5\text{Cl}_1\text{H}_5\text{H}$	296.1
$\text{CB}_4\text{Cl}_4\text{H}_1\text{H}$	289.6	$\text{CB}_5\text{Cl}_5\text{H}_1\text{H}$	268.1
$\text{CB}_4\text{Cl}_5\text{H}$	284.1	$\text{CB}_5\text{Cl}_6\text{H}$	262.7
$\text{CB}_4(\text{CF}_3)_1\text{H}_4\text{H}$	300.1	$\text{CB}_5(\text{CF}_3)_1\text{H}_5\text{H}$	288.8
$\text{CB}_4(\text{CF}_3)_4\text{H}_1\text{H}$	257.1	$\text{CB}_5(\text{CF}_3)_5\text{H}_1\text{H}$	235.7
$\text{CB}_4(\text{CF}_3)_5\text{H}$	245.7	$\text{CB}_5(\text{CF}_3)_6\text{H}$	227.0

Table 2. ΔG_{acid} values (kcal/mol) of $\text{CB}_4\text{F}_5\text{H}$ and $\text{CB}_5\text{F}_6\text{H}$ based systems calculated at the DFT B3LYP/6-31+G* level (298 K)

1 : 3 : 1 acid	ΔG_{acid}	1 : 4 : 1 acid	ΔG_{acid}
$\text{CB}_4\text{H}_5\text{H}$	318.5	$\text{CB}_5\text{H}_6\text{H}$	304.0
$\text{CB}_4\text{F}_1\text{H}_4\text{H}$	313.8	$\text{CB}_5\text{F}_1\text{H}_5\text{H}$	300.9
$\text{CB}_4\text{F}_4\text{H}_1\text{H}$	305.1	$\text{CB}_5\text{F}_5\text{H}_1\text{H}$	283.5
$\text{CB}_4\text{F}_5\text{H}$	301.8	$\text{CB}_5\text{F}_6\text{H}$	277.9

THE SYSTEMS BASED ON CB_4H_5^- ANION

$\text{CB}_4\text{X}_n\text{H}_{5-n}\text{H}$ ($\text{X} \equiv \text{F}; \text{Cl}; \text{CF}_3$) with different degrees of substitution were the smallest systems calculated, consisting of two base-coupled tetrahedrons with heights of 1.1 Å ($\text{C}_1\text{B}_2\text{B}_3\text{B}_4$) and 1.3 Å ($\text{B}_1\text{B}_2\text{B}_3\text{B}_4$) (Fig. 1).

The influence of the substituents varied mostly by the extent of deformation of the anion, depending on the type and amount of the substituents. Comparison of the systems according to the degree of substitution revealed that addition of a single charged acceptor had no substantial influence on the geometry. Replacement of all B–H groups with B–X groups made the systems somewhat wider increasing the distance between the middle-belt boron atoms up to 0.1 Å. When fluorine substituents were used, the widening was more noticeable compared to chlorine or CF_3 substituents.

The following protonation sites were investigated: near the B_1 vertex, near the triangular facet $\text{B}_1\text{B}_2\text{B}_4$, near the triangular facet $\text{B}_3\text{B}_4\text{C}_5$, and

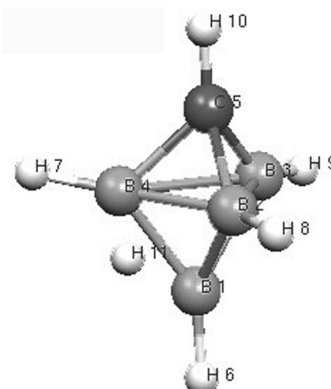


Fig. 1. $\text{CB}_4\text{X}_n\text{H}_{5-n}\text{H}$ systems.

near the C₅ vertex of the cage. Energetically the most favourable protonated form was the one with the proton on the B₁B₂B₄ facet, shifted towards the B₁–B₄ bond. The corresponding distances between hydrogen ion and both B₁ and B₄ were about 1.3–1.4 Å and B₂ 2.1–2.3 Å. Differences in energy, comparing the intramolecular protonation sites, remained mostly between 10 and 15 kcal/mol. Larger variation occurred with fully substituted forms giving an approximately 25 kcal/mol difference with CB₄(CF₃)₅H.

Protonation to the outer sphere between or on the substituents led to the disintegration of the molecule.

THE SYSTEMS BASED ON CB₅H₆[−] ANION

The second species consisted of two base-coupled square pyramids, B₁–C₆ distance 1.6 Å. With CB₅X_nH_{6−n}H systems, the following protonation (H13) sites were explored (Fig. 2): near the B₁ vertex, near the B₁B₂B₃ facet, near the B₂B₅C₆ facet, and near the C₆ vertex. Energetically the most favourable protonation centre, throughout different substitution levels, was the B₁B₂B₃ facet, about 1.33–1.37 Å from B₂ and B₃ equally and quite invariably, and 1.6–2.1 Å from B₁, antipodal to carbon.

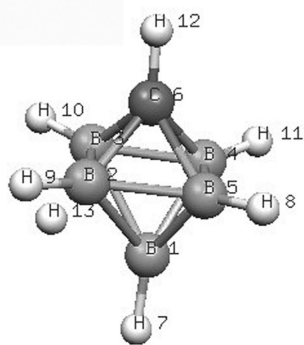


Fig. 2. CB₅H_nH_{6−n}H systems.

The addition of charge-withdrawing groups had practically no effect on the structure. The B–B distances remained around 1.7 Å.

Bond lengths, in the case of addition of the hydrogen ion, were strained up to 0.3 Å between antipodal B₁ and middle-belt vertexes on the protonated facet of the cage. The distances on the opposing side of the pyramid remained around 1.6 Å, as they were also in the anion.

Describing the differences in energies of the different protonation sites using the obtained results would not make much sense, because during the geometry optimizations the proton drifted always to the same place. The corresponding distances were: B₂H⁺ 1.4 Å, B₃H⁺ 1.4 Å, and B₅H⁺ 1.7 Å.

The exceptions were the fully fluorinated and chlorinated systems, showing a tendency to break if the proton was placed at the same side with the carbon vertex.

DISCUSSION

The calculated intrinsic acidities of the derivatives of CB₄X_nH_{5−n}H and CB₅X_nH_{6−n}H cover ΔG_{acid} values from above sulphuric acid down to the strongest acids known, placing CB₅(CF₃)₆H to about 18 kcal/mol above the classic CB₁₁F₁₂H (Fig. 3) [10, 11]. The main factor responsible for the very high acidity is the charge

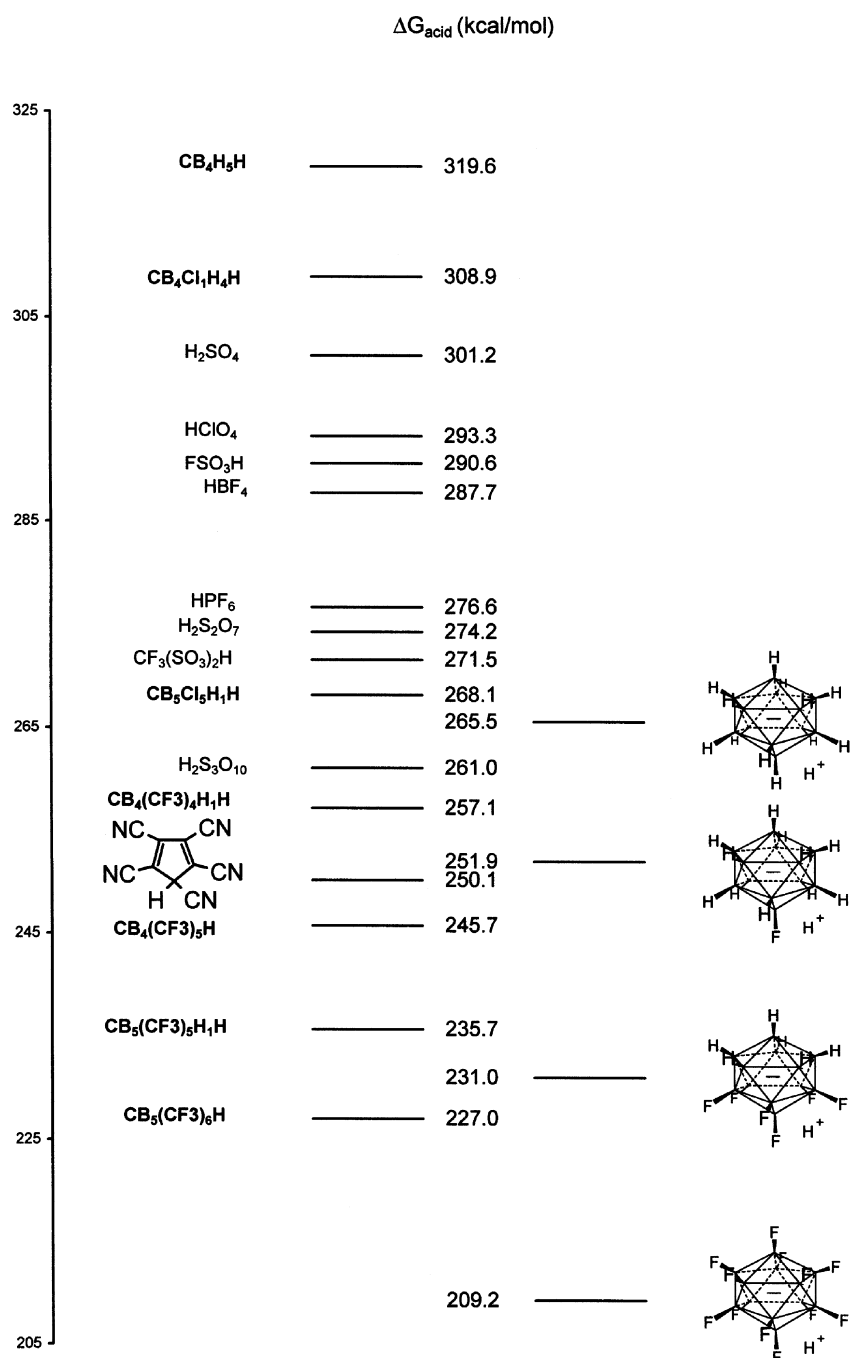


Fig. 3. Computational gas-phase superacidity ladder including some carborane acids presented in kcal/mol. All systems are calculated at 6-311+G**, except the derivatives of CB₁₁H₁₂H, which are calculated at the 6-31+G* level. The data for mineral acids, C₅H(CN)₅, and derivatives of CB₁₁H₁₂H were taken from [11]. Compound names calculated in the present study are written in bold.

withdrawing effect of the electron acceptor groups. Nevertheless, this could also be the reason why substituted species tend to be fairly unstable [13, 14], if smaller and “harder” fluorine or chlorine groups were used, as $\text{CB}_4\text{X}_n\text{H}_{5-n}\text{H}$ ($\text{X} \equiv \text{F}$ or Cl) anion structures tended to be somewhat disturbed when the proton was added, but at the same time CF_3 -substituted systems remained completely intact.

The clusters without substituent groups were found to have quite modest acidity, both systems staying above 300 kcal/mol. Addition of a single acceptor into the antipodal position to carbon led in each case to a small increase in acidities having the maximum value of roughly 20 kcal/mol with the CF_3 group (Fig. 4). The main increase was obtained when all vertexes but carbon were covered yielding ΔG_{acid} values around 10 kcal/mol above the species that were fully substituted.

Considering the results from previous works [11, 12, 15] it could be assumed that the most suitable protonation site would be between two substituents of the B–X groups, which are on the opposite polyhedron from the carbon. Nevertheless the most favourable site for proton was near the boron vertexes. The reason is probably that one B–X group is not able to stabilize the ion and the distance between two electron-withdrawing groups is too large (ca 4 Å) to have preferred bidentate interaction, so the most stable form left is the one with the proton placed between the middle-belt and the topmost boron in the case of 1:3:1 systems and between two middle-belt borons in the case of 1:4:1 clusters.

As a rule the protonation mechanisms of the $\text{CB}_4\text{X}_n\text{H}_{5-n}\text{H}$ and $\text{CB}_5\text{X}_n\text{H}_{6-n}\text{H}$ systems were found to be different. With smaller cages the boron atoms of the middle-belt and antipodal vertex attracted the proton most, yielding the strongest interactions with almost 10 kcal/mol higher than the one just protonated to the

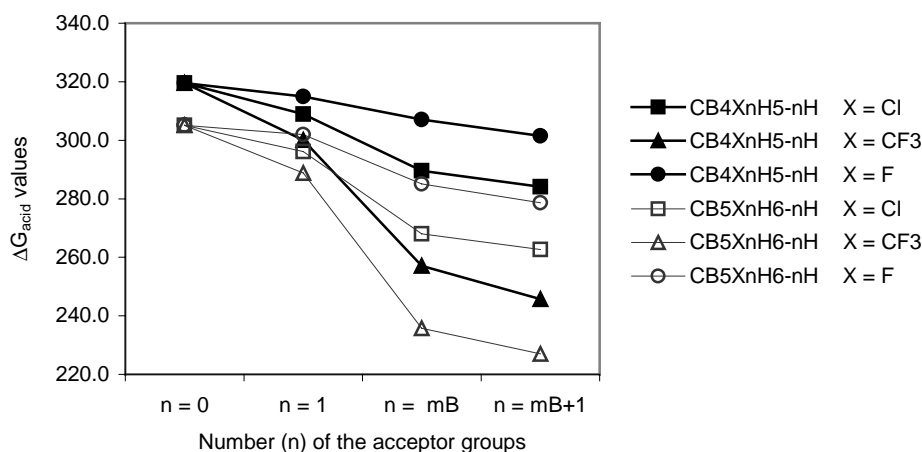


Fig. 4. Comparison of the intrinsic acidities of carborane acids according to addition of substituents; mB is the number of boron vertexes in the cluster.

antipodal boron. The side-effect was that the bond between the nearest middle-belt boron atoms was lengthened from about 1.8 Å to 2.1 Å. With the larger cage about 0.3 Å stretching occurred with the distances between the antipodal boron and the middle-belt boron, while the bond between the middle-belt boron atoms had changed only around 0.1 Å.

In general the $\text{CB}_5\text{X}_n\text{H}_{6-n}\text{H}$ cluster retained somewhat better its shape originating from the anion, especially if $\text{B}-\text{CF}_3$ groups were used instead of $\text{B}-\text{F}$ or $\text{B}-\text{Cl}$.

For comparison the fluorinated systems were calculated also at the 6-31+G* level, yielding results in ΔG_{acid} values that differed from the higher level calculations by only 1–2 kcal/mol (Table 2).

CONCLUSIONS

In this study the effect of F-, Cl-, and CF_3 -substituents on the acidities of the smallest carborane acids calculated so far were investigated. The ΔG_{acid} values ranged from above common sulphuric acid values down to the half-fluorinated acid form of 1-carba-*closo*-dodecaborate. The acidity-increasing effect of the studied substituents increased in the order $\text{F} < \text{Cl} < \text{CF}_3$. Also the size of the anion has its role but mostly because of the possibility of adding more substituents.

The most favourable protonation site for both systems studied was on the facet that was on the opposite side of the molecule if taken from the carbon. The exact position varied though, being between the antipodal boron and the middle-belt boron in the case of $\text{CB}_4\text{X}_n\text{H}_{5-n}$ and between the two middle-belt vertexes in the case of $\text{CB}_5\text{X}_n\text{H}_{6-n}$ systems.

Although mainly the DFT B3LYP method at the 6-311+G** level was used, the results with the 6-31+G* basis set are also fully adequate, and the use of the latter for the larger systems would be quite reasonable.

ACKNOWLEDGEMENT

This work was supported by grant 6701 from the Estonian Science Foundation.

APPENDIXES

Appendix 1. Results of DFT B3LYP calculations of $\text{CB}_4\text{X}_n\text{H}_{5-n}\text{H}$ type systems at the 6-311+G** level

1 : 3 : 1 input geometries	N_{imag}	E^a	H (298 K) ^a	G (298 K) ^a	ΔH , kcal/mol	ΔG , kcal/mol
CB_4H_5^-	0	-140.5861	-140.5154	-140.5463		
H ⁺ on the BBB facet	0	-141.1150	-141.0330	-141.0656	326.3	319.6
H ⁺ on the B ₅ -B bond	0	-141.1150	-141.0329	-141.0656	326.3	319.6
H ⁺ on the BCB facet	0	-141.0834	-141.0015	-141.0350	306.5	300.4
“Fishtale” on B ₅ vertex	0	-141.0989	-141.0199	-141.0519	318.1	311.0
$\text{CB}_4\text{H}_4\text{F}^-$	0	-239.9140	-239.8484	-239.8819		
H ⁺ on the BBB facet	0	-240.4353	-240.3583	-240.3937	321.5	314.9
H ⁺ on the B ₅ -B bond	0	-240.4353	-240.3583	-240.3937	321.5	314.9
H ⁺ on the BCB facet	0	-240.4117	-240.3348	-240.3703	306.7	300.2
$\text{CB}_4\text{F}_4\text{H}^-$	0	-537.9094	-537.8589	-537.9004		
H ⁺ on the BBB facet	0	-538.4175	-538.3560	-538.3997	313.4	307.1
H ⁺ on the B ₅ -B bond	0	-538.4164	-538.3547	-538.3983	312.6	306.2
H ⁺ on the BCB facet	0	-538.4001	-538.3381	-538.3817	302.2	295.8
H ⁺ on the middle-belt F	0	HF separated, optimization broke the cage				
CB_4F_5^-	0	-637.1638	-637.1198	-637.1655		
H ⁺ on the BBB facet	0	-637.6617	-637.6069	-637.6533	307.1	299.8
H ⁺ on the B ₅ -B bond	0	-637.6660	-637.6107	-637.6561	309.5	301.5
H ⁺ on the BCB facet	0	-637.6491	-637.5938	-637.6397	298.9	291.3
H ⁺ on the F of antipodal vertex	0	-637.5768	-637.5214	-637.5697	253.5	247.3
H ⁺ on the middle-belt F	0	HF separated, optimization broke the cage				
$\text{CB}_4\text{H}_4\text{Cl}^-$	0	-600.2667	-600.2016	-600.2365		
H ⁺ on the BBB facet	0	-600.7782	-600.7023	-600.7388	315.6	308.9
H ⁺ on the BCB facet	0	-600.7542	-600.6782	-600.7152	300.5	294.1
$\text{CB}_4\text{Cl}_4\text{H}^-$	0	-1979.3036	-1979.2559	-1979.3023		
H ⁺ on the B ₅ -B bond	0	-1979.7834	-1979.7256	-1979.7739	296.2	289.6
H ⁺ on the BBB facet	0	-1979.7818	-1979.7246	-1979.7736	295.6	289.4
H ⁺ on the BCB facet	0	-1979.7604	-1979.7026	-1979.7514	281.8	275.5
CB_4Cl_5^-	0	-2438.9262	-2438.8861	-2438.9364		
H ⁺ on the B ₅ -B bond	0	-2439.3976	-2439.3475	-2439.3992	291.0	284.1
H ⁺ on the BBB facet	0	-2439.3942	-2439.3448	-2439.3976	289.3	283.1
H ⁺ on the BCB facet	0	-2439.3667	-2439.3168	-2439.3695	271.8	265.5
$\text{CB}_4\text{H}_4\text{CF}_3^-$	0	-477.7703	-477.6898	-477.7319		
H ⁺ on the BBB facet	0	-478.2683	-478.1766	-478.2202	307.0	300.1
H ⁺ on the BCB facet	0	-478.2399	-478.1484	-478.1941	289.3	283.8
$\text{CB}_4\text{H}_4(\text{CF}_3)_4^-$	0	-1489.2825	-1489.1726	-1489.2479		
H ⁺ on the BBB facet	0	-1489.7121	-1489.5916	-1489.6676	264.4	257.1
H ⁺ on the BCB facet	0	-1489.6874	-1489.5674	-1489.6451	249.2	243.0
$\text{CB}_4\text{H}_4(\text{CF}_3)_5^-$	0	-1826.4377	-1826.3193	-1826.4036		
H ⁺ on the BBB facet	0	-1826.8491	-1826.7202	-1826.8052	253.1	245.7
H ⁺ on the BCB facet	0	-1826.8103	-1826.6815	-1826.7659	228.7	221.0

^a Given in Hartrees. 1 Hartree = 627.5 kcal/mol; E is the HF energy at °K, without ZPV correction, H refers to enthalpies and G to Gibbs free energies. N_{imag} shows the amount of imaginary frequencies.

Appendix 2. Results of DFT B3LYP calculations of $\text{CB}_5\text{X}_n\text{H}_{6-n}\text{H}$ type systems at the 6-311+G** level

1 : 4 : 1 input geometries	N_{imag}	E^a	H (298 K) ^a	G (298 K) ^a	ΔH , kcal/mol	ΔG , kcal/mol
CB_5H_6^-	0	-166.1011	-166.0138	-166.0471		
H ⁺ on the BBB facet	0	-166.6073	-166.5094	-166.5433	312.5	305.1
H ⁺ on the BCB facet	0	-166.6073	-166.5094	-166.5432	312.4	305.1
$\text{CB}_5\text{H}_5\text{F}^-$	0	-265.4333	-265.3511	-265.3866		
H ⁺ on the BBB facet	0	-265.9345	-265.8415	-265.8778	309.2	301.9
on C–B bond	0	-265.9346	-265.8415	-265.8777	309.2	301.9
H ⁺ on the BCB facet	0	-265.9345	-265.8415	-265.8778	309.2	301.9
$\text{CB}_5\text{F}_5\text{H}^-$	0	-662.7349	-662.6739	-662.7194		
H ⁺ on the BBB facet	0	-663.2095	-663.1377	-663.1837	292.5	285.1
on C–B bond	0	-663.2095	-663.1376	-663.1836	292.5	285.0
H ⁺ on the BCB facet	0	-663.2095	-663.1377	-663.1837	292.5	285.1
CB_5F_6^-	0	-761.9869	-761.9326	-761.9809		
H ⁺ on the BBB facet	0	-762.4511	-762.3863	-762.4349	286.1	278.6
H ⁺ on the BCB facet	0	The cage disintegrated				
on C–B bond	0	The cage disintegrated				
H ⁺ on the middle-belt F	0	-762.3679	-762.3032	-762.3519	234.0	226.5
H ⁺ on the middle-belt F	2	-762.3693	-762.3058	-762.3535	235.7	227.5
$\text{CB}_5\text{H}_5\text{Cl}^-$	0	-625.7821	-625.7007	-625.7376		
H ⁺ on the BBB facet	0	-626.2737	-626.1818	-626.2195	303.4	296.1
H ⁺ on the BCB facet	0	-626.2737	-626.1818	-626.2195	303.4	296.1
on C–B bond	1	-626.2219	-626.1326	-626.1703	272.5	265.3
$\text{CB}_5\text{Cl}_5\text{H}^-$	0	-2464.4781	-2464.4207	-2464.4727		
H ⁺ on the BBB facet	0	-2464.9242	-2464.8574	-2464.9099	275.5	268.1
H ⁺ on the BCB facet	0	-2464.9242	-2464.8574	-2464.9099	275.5	268.1
CB_5Cl_6^-	0	-2924.0966	-2924.0471	-2924.1026		
H ⁺ on the BBB facet	0	-2924.5341	-2924.4753	-2924.5313	270.2	262.7
H ⁺ on the BCB facet	0	-2924.5236	-2924.4648	-2924.5227	263.6	257.3
on B ₆ –B bond	0	-2924.5341	-2924.4753	-2924.5313	270.2	262.7
$\text{CB}_5\text{H}_5\text{CF}_3^-$	0	-503.2806	-503.1838	-503.2282		
H ⁺ on the BBB facet	0	-503.7597	-503.6523	-503.6985	295.5	288.8
H ⁺ on the BCB facet	0	-503.7597	-503.6523	-503.6985	295.5	288.8
$\text{CB}_5(\text{CF}_3)_5\text{H}^-$	0	-1851.9511	-1851.8158	-1851.9028		
H ⁺ on the BBB facet	0	-1852.3461	-1852.2010	-1852.2884	243.2	235.7
H ⁺ on the BCB facet	0	-1852.3461	-1852.2010	-1852.2884	243.2	235.7
$\text{CB}_5(\text{CF}_3)_6^-$	0	-2189.0953	-2188.9520	-2189.0477		
H ⁺ on the BBB facet	0	-2189.4760	-2189.3230	-2189.4189	234.3	226.6
H ⁺ on the BCB facet	0	-2189.4762	-2189.3231	-2189.4196	234.3	227.0

^a See the footnote to Appendix 1.

REFERENCES

1. Strauss, S. H. The search for larger and more weakly coordinating anions. *Chem. Rev.*, 1993, **93**, 927–942.
2. Krossing, I. & Raabe, I. Noncoordination anions – fact or fiction? A survey of likely candidates. *Angew. Chem., Int. Ed.*, 2004, **43**, 2066–2090.

3. Reed, A. C. Carboranes: a new class of weakly coordinating anions for strong electrophiles, oxidants, and superacids. *Acc. Chem. Res.*, 1998, **31**, 133–139.
4. Knoth, W. H. $1\text{-B}_9\text{H}_9\text{CH}^-$ and $\text{B}_{11}\text{H}_{11}\text{CH}^-$. *J. Am. Chem. Soc.*, 1967, **89**, 1274–1275.
5. Plešek, J., Jelínek, T., Drdáková, E., Heřmánek, S. & Štíbr, B. A convenient preparation of $1\text{-CB}_{11}\text{H}_{12}^-$ and its C-amino derivatives. *Collect. Czech. Chem. Commun.*, 1984, **49**, 1559–1562.
6. King, B. T., Zharov, I. & Michl, J. Alkylated carborane anions and radicals: tools for organic and inorganic chemists. *Chem. Innov.*, 2001, **12**, 23–31.
7. Reed, C. A., Kim, K.-C., Bolskar, R. D. & Mueller, L. Taming superacids: stabilization of the fullerene cations HC_{60}^+ and C_{60}^+ . *Science*, 2000, **289**, 101–104.
8. Juhasz, M., Hoffmann, S., Stoyanov, E., Kim, K.-C. & Reed, C. A. The strongest isolable acid. *Angew. Chem., Int. Ed.*, 2004, **43**, 5352–5355.
9. Reed, C. A. Carborane acids. New “strong yet gentle” acids for organic and inorganic chemistry. *Chem. Commun.*, 2005, 1669–1677.
10. Koppel, I., Lipping, L., Leito, I., Burk, P., Mishima, M. & Sonoda, T. Carborane derivatives – the least coordinating anions and the strongest acids. In *KISPOC 9 Symposium, Book of Abstracts*. Fukuoka, 2001, 183–186.
11. Koppel, I. A., Burk, P., Koppel, I., Leito, I., Sonoda, T. & Mishima, M. Gas-phase acidities of some neutral Brønsted superacids: a DFT and ab initio study. *J. Am. Chem. Soc.*, 2000, **122**, 5114–5124.
12. Stoyanov, E. S., Hoffmann, S. P., Juhasz, M. & Reed, C. A. The structure of the strongest Brønsted acid $\text{H}(\text{CHB}_{11}\text{Cl}_{11})$. *J. Am. Chem. Soc.*, 2006, **128**, 3160–3161.
13. King, B. T. & Michl, J. The explosive “inert” anion $\text{CB}_{11}(\text{CF}_3)_{12}^-$. *J. Am. Chem. Soc.*, 2000, **122**, 10255–10256.
14. Stasko, D. & Reed, C. A. Optimizing the least nucleophilic anion. A new, strong methyl⁺ reagent. *J. Am. Chem. Soc.*, 2002, **124**, 1148–1149.
15. Balarayan, P. & Gadre, S. H. Why are carborane acids so acidic? An electrostatic interpretation of Brønsted acid strengths. *Inorg. Chem.*, 2005, **44**, 9613–9615.

Mõned karboraanidel baseeruvad superhapped

Lauri Lipping, Ilmar A. Koppel, Ivar Koppel ja Ivo Leito

Gaasifaasilised happelisused on arvatatud $\text{CB}_4\text{X}_n\text{H}_{5-n}\text{H}^-$ ja $\text{CB}_5\text{X}_n\text{H}_{6-n}^-$ tüüpi süsteemide jaoks ($\text{X} \equiv \text{F}, \text{Cl}$ või CF_3) DFT B3LYP hübriidse meetodiga 6-311+G** tasemel. Võrdluseks on arvatatud 6-31+G* baasiga samad süsteimid ainult fluor-asendusühmade jaoks. Mõlema arvutusmeetodi tulemused korreleeruvad omavahel rahuldavalt. Töö käigus on määratud soodsaim protoneerumissenter vastavas happes. Selleks osutub süsiniku suhtes antipodaalse püramidaalse osa üks tahk. Võrreldes asendusühmi vastavalt nende mõjule karboraanhappe happelisusele, on saadud järjestus $\text{F} < \text{Cl} < \text{CF}_3$.